LPV force observer design and experimental validation from a dynamical semi-active ER damper model ⋆

Thanh-Phong Pham [*,**] **Olivier Sename** [*] **Luc Dugard** [*]
Van Tan Vu [***]

[*] *Univ. Grenoble Alpes, CNRS, Grenoble INP*[⊤]*, GIPSA-lab, 38000 Grenoble, France.* [⊤] *Institute of Engineering Univ. Grenoble Alpes (e-mail: thanh-phong.pham2, olivier.sename, luc.dugard@ gipsa-lab.grenoble-inp.fr).*
[**] *Faculty of Electrical and Electronic Engineering, The University of Danang - University of Technology and Education, 550000 Danang, Vietnam*
[***] *Department of Automotive Mechanical Engineering, University of Transport and Communications, Hanoi, Vietnam. (e-mail: vvtan@utc.edu.vn)*

Abstract: This paper presents an LPV damping force observer of ElectroRheological (ER) dampers for a real automotive suspension system, taking the dynamic characteristic of damper into account. First, an extended nonlinear quarter-car model is considered, where the time constant representing the damper dynamics is varying according to the control level. This is rewritten as an LPV model which is used to design an LPV observer. The objective of the LPV observer is to minimize the effects of bounded unknown input disturbances (unknown road profile and measurement noises) on the state estimation errors through an $\mathcal{H}_\infty$ criterion, while the damper nonlinearity is bounded using a Lipschitz condition. Two low-cost accelerometers (the sprung mass and the unsprung mass accelerations) are used as inputs for the proposed methodology only. To experimentally assess the proposed approach, it is implemented on the 1/5-scaled real vehicle-INOVE testbench of GIPSA-lab. This shows the ability of the observer to estimate the damper force in real-time, face to unknown inputs disturbance and sensor noises.

Keywords: LPV Observer, Semi-active suspension, Electrorheological damper, Lipchitz nonlinearity, damping force estimation,

1. INTRODUCTION

Nowadays, the semi-active damper for automotive suspension systems is one of the key components which improves safety and comfort for on-board passengers. Therefore, it has received a lot of attention from industry and academia (Savaresi et al. (2010) and references therein). Several control methods were proposed in the literature (see a review in Poussot-Vassal et al. (2012)). Based on the implementation aspects, these methods can be broadly classified into: a) use of an inverse model or look-up tables (Poussot-Vassal et al. (2008), Do et al. (2010), Nguyen et al. (2015)) and b) use of an inner force tracking controller (Priyandoko et al. (2009), Aubouet (2010)). However, as damper force sensors are expensive and difficult to install in practice, the real-time estimation of the damper force is of paramount importance for suspension control.

The key requirements for designing damper force observer are to use classical on-board sensors (such as accelerometers), to take into account the nonlinear dynamical behavior of the damper and to handle sensor noises and unknown road profile disturbances. To this aim, several estimation methodologies were proposed. Some are only considering a static damper model such as the Kalman filter presented in (Koch et al. (2010)). In order to consider the dynamical characteristic of the damper, robust observers (H_∞, LPV-H_∞, H_∞ Lipschitz and unified H_∞ observers) were proposed in Estrada-Vela et al. (2018), Tudon-Martinez et al. (2018), Pham et al. (2019a), Pham et al. (2019b). Although the estimation methodologies provide interesting results, the varying time constant of the dynamical nonlinear model has been ignored as far as we know.

In this paper, we aim first to extend the estimation method in Pham et al. (2019a) to *LPV* systems in order to deal with the varying time constant of the damper. An *LPV* observer is then developed to estimate the damper force of the suspension system in real-time, using two accelerometers only. The major contributions of this paper are as follows:

⋆ This work has been partially supported by the 911 scholarship from Vietnamese government. The authors also thank the financial support of the ITEA3 European Project through EMPHYSIS (Embedded Systems With Physical Models in the Production Code Software) under Grant 15016.

- A quarter-car suspension nonlinear model is augmented with a first order nonlinear dynamical damper model and is rewritten as an LPV model for which the scheduling variable is the damper time constant (modelled by a polynomial function of the control input).
- A polytopic LPV approach for Lipchitz nonlinear system is developed to design an observer minimizing, in an $\mathcal{L}_2$-induced gain objective, the effect of unknown inputs (road profile and measurement noises) and to dealing with the varying of the time constant in the dynamic model.
- The proposed observer has been implemented on a real scaled-vehicle test bench, through the Matlab/Simulink Real-Time Workshop to experimentally assesses the performance of the observer.

The rest of this paper is organized as follows. Section 2 presents the semi-active damper modeling and quarter-car system description and section 3 the design of the LPV observer. In section 4 and 5, simulation and experimental results are shown, respectively. Section 5 gives some concluding remarks.

2. SEMI-ACTIVE DAMPER MODELING AND QUARTER-CAR SYSTEM DESCRIPTION

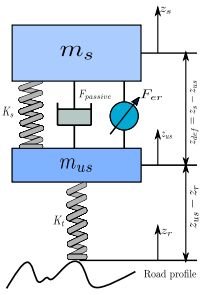


Fig. 1. 1/4 car model with semi-active suspension

2.1 Physical model and identification

This section introduces the quarter-car model including the semi-active ER suspension system depicted in Fig.1. The well-known model consists of the sprung mass (m_s), the unsprung mass (m_{us}), the suspension components (spring with stiffness k_s and damper) located between (m_s) and (m_{us}) and the tire which is modelled as a spring with stiffness k_t. From Newton's second law of motion, the system dynamics around the equilibrium are given as:

$$\begin{cases} m_s\ddot{z}_s & = -F_s - F_d \\ m_{us}\ddot{z}_{us} & = F_s + F_d - F_t \end{cases} \tag{1}$$

In (1), the spring force F_s and the tire force F_t are given as follows:

$$\begin{aligned} F_s &= k_s(z_s - z_{us}) \\ F_t &= k_t(z_{us} - z_r) \end{aligned} \tag{2}$$

where z_s and z_{us} are the displacements of the sprung and unsprung masses, respectively; z_r is the road displacement input.

Let us now describe the proposed semi-active damper modelling method. First following Guo et al. (2006), a phenomenological damper model is expressed as

$$\begin{cases} F_d & = k_0(z_s - z_{us}) + c_0(\dot{z}_s - \dot{z}_{us}) + F_{nl} \\ F_{nl} & = f_c \cdot u \cdot tanh(k_1(z_s - z_{us}) + c_1(\dot{z}_s - \dot{z}_{us})) \end{cases} \tag{3}$$

where F_d is the damper force; c_0, c_1, k_0, k_1, f_c are constant parameters. In the ER damper, the control input u is the voltage input that provides the electrical field to control the ER damper. In practice, it is the duty cycle of the PWM signal that controls the application.

However, the above model does not consider the dynamical damper behavior, while, for semi-active dampers, it is known to be an important issue for modelling and control (see Koo et al. (2006)).

In order to take into account the varying dynamical behavior of the ER fluid, the above model (3) is completed by a first-order dynamical equation of the controlled part F_{nl}:

$$\tau(u)\dot{F}_{er} + F_{er} = F_{nl} \tag{4}$$

Therefore, the complete nonlinear dynamical model is given as

$$\begin{cases} F_d & = k_0(z_s - z_{us}) + c_0(\dot{z}_s - \dot{z}_{us}) + F_{er} \\ F_{nl} & = f_c \cdot u \cdot tanh(k_1(z_s - z_{us}) + c_1(\dot{z}_s - \dot{z}_{us})) \\ \tau(u)\dot{F}_{er} & = -F_{er} + F_{nl} \end{cases} \tag{5}$$

According to Koo et al. (2006), the varying time constant $\tau(u)$ depends on the control input u and can be identified following the next steps.

In order to identify $\tau(u)$, the experimental tests considered the velocity input within the range $[-0.15\,,\,0.15]\,\frac{\text{m}}{\text{s}}$ and the fixed PWM (i.e. u_{eq}) signals inside the set $\{0\,,10\,,15\,,20\,,25\,,30\}\,\%$. The identification process is then divided into both following steps:
Step 1: During each experimental test with a constant value u_{eq}, the corresponding force F_{er} is obtained from the test bed force sensor (see section 5) while F_{nl} is calculated based on the static model of ER damper. Then, the fixed time constant $\tau(u_{eq})$ can be identified by using Least Squares method. Finally, the set of time constants τ for all u_{eq} is shown in Table 1.

Table 1. Values of time constant τ with different PWM signals

PWM	τ	Unit
0	0	ms
0.1	0.0137	s
0.15	0.0221	s
0.2	0.0365	s
0.25	0.055	s
0.3	0.0631	s

Step 2: Based on the values in Table 1, the relationship between τ and u can be approximated by the following polynomial function (Figure 2)

$$\tau(u) = 0.3643u^2 + 0.1124u \tag{6}$$

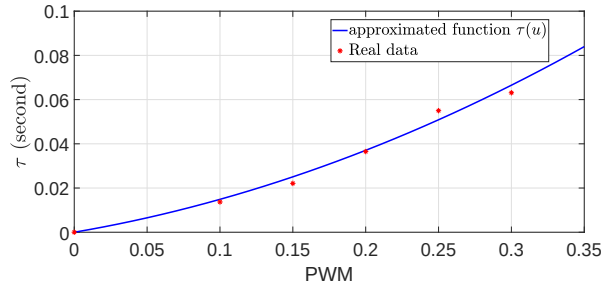


Fig. 2. The relation between τ and u

It is noted that linear and nonlinear identification methodologies are used to determine all the parameters of the model (3) (shown in table 2). They are not described here since it is out of the scope of this paper.

Table 2. Parameter values of the quarter-car model equipped with an ER damper

Parameter	Description	value	Unit
m_s	Sprung mass	2.27	kg
m_{us}	unsprung mass	0.25	kg
k_s	Spring stiffness	1396	N/m
k_t	Tire stiffness	12270	N/m
k_0	Passive damper stiffness coefficient	170.4	N/m
c_0	Viscous damping coefficient	68.83	N.s/m
k_1	Hysteresis coefficient due to displacement	218.16	N.s/m
c_1	Hysteresis coefficient due to velocity	21	N.s/m
f_c	Dynamic yield force of ER fluid	28.07	N

2.2 LPV modelling

In this section, the quarter-car system is rewritten into the LPV form for observer design.

By selecting the system states as $x = [x_1, x_2, x_3, x_4, x_5]^T = [z_s - z_{us}, \dot{z}_s, z_{us} - z_r, \dot{z}_{us}, F_{er}]^T \in \mathbb{R}^5$, the measured variables $y = [\ddot{z}_s, \ddot{z}_{us}]^T \in \mathbb{R}^2$ and the scheduling variable $\rho = \frac{1}{\tau(u)} \in \mathbb{R}$, the system dynamics can be written in the following LPV form:

$$\begin{cases} \dot{x} &= A(\rho)x + B(\rho)\Phi(x)u + D_1\omega \\ y &= Cx + D_2\omega \end{cases} \tag{7}$$

where $\omega = \begin{pmatrix} \dot{z}_r \\ n \end{pmatrix}$, in which, $\dot{z}_r$ is the road profile derivative and n is the sensor noises.

$$\begin{aligned} \Phi(x) &= tanh(k_1x_1 + c_1(x_2 - x_4)) \\ &= tanh(\Gamma x) \end{aligned}$$

with $\Gamma = [k_1,\ c_1,\ 0,\ -c_1,\ 0]$

$$A = \begin{bmatrix} 0 & 1 & 0 & -1 & 0 \\ -\frac{(k_s+k_0)}{m_s} & -\frac{c_0}{m_s} & 0 & \frac{c_0}{m_s} & -\frac{1}{m_s} \\ 0 & 0 & 0 & 1 & 0 \\ \frac{(k_s+k_0)}{m_{us}} & \frac{c_0}{m_{us}} & -\frac{k_t}{m_{us}} & -\frac{c_0}{m_{us}} & \frac{1}{m_{us}} \\ 0 & 0 & 0 & 0 & -\rho \end{bmatrix}$$

$$C = \begin{bmatrix} -\frac{(k_s+k_0)}{m_s} & -\frac{c_0}{m_s} & 0 & \frac{c_0}{m_s} & -\frac{1}{m_s} \\ \frac{(k_s+k_0)}{m_{us}} & \frac{c_0}{m_{us}} & -\frac{k_t}{m_{us}} & -\frac{c_0}{m_{us}} & \frac{1}{m_{us}} \end{bmatrix}$$

$$B = \begin{bmatrix} 0 \\ 0 \\ 0 \\ 0 \\ f_c \cdot \rho \end{bmatrix}, D_1 = \begin{bmatrix} 0 & 0 \\ 0 & 0 \\ -1 & 0 \\ 0 & 0 \\ 0 & 0 \end{bmatrix}, D_2 = \begin{bmatrix} 0 & 0.01 \\ 0 & 0.01 \end{bmatrix}$$

Remark: Since control input signal u are accessible in observer design, the scheduling variable $\rho = \frac{1}{\tau(u)}$ is known online via the function of control input signal u and τ (6).

According to Apkarian et al. (1995), since the scheduling parameter ρ varies in a polytope $\mathcal{Y}$ of 2 vertices $\rho \in [\underline{\rho}, \overline{\rho}]$, the matrices $A(\rho)$, $B(\rho)$ can be transformed into a convex interpolation as follows:

$$A(\rho) = \sum_{i=1}^{2} \alpha_i(\rho)A_i, \quad B(\rho) = \sum_{i=1}^{2} \alpha_i(\rho)B_i \tag{8}$$

$$\alpha_i(\rho) \geqslant 0, \quad \sum_{i=1}^{2} \alpha_i(\rho) = 1, \tag{9}$$

where $A_1 = A(\underline{\rho})$, $A_2 = A(\overline{\rho})$, $B_1 = B(\underline{\rho})$, $B_2 = B(\overline{\rho})$

3. *LPV* OBSERVER DESIGN

In this section, a polytopic *LPV* observer is proposed to estimate the ER damper force accurately. An H_∞ criterion is used to minimize the effect of the unknown disturbance ω on the state estimation errors and to bound the nonlinearity by Lipschitz constant.

The considered problem is to estimate the damper force F_d. Following the modelling step above, the estimated force $\hat{F}_d$ is then defined as:

$$\hat{F}_d = k_0\hat{x}_1 + c_0(\hat{x}_2 - \hat{x}_4) + \hat{x}_5 \tag{10}$$

Therefore, the state variables to be accurately estimated by the observer are representing by the vector $z = [x_1, x_2, x_4, x_5]^T \in \mathbb{R}^4$.

The polytopic *LPV* observer for the quarter-car system (7) has the following structure:

$$\begin{cases} \dot{\hat{x}} = A(\rho)\hat{x} + L(\rho)(y - C\hat{x}) + B(\rho)\Phi(\hat{x})u \\ \hat{z} = C_z\hat{x} \end{cases} \tag{11}$$

where $\hat{x}$ is the estimated states of the states x, $\hat{z}$ is the estimated variables of the variables z and $C_z = \begin{bmatrix} 1 & 0 & 0 & 0 & 0 \\ 0 & 1 & 0 & 0 & 0 \\ 0 & 0 & 0 & 1 & 0 \\ 0 & 0 & 0 & 0 & 1 \end{bmatrix}$.

The observer gains $L(\rho)$ to be determined in the next steps are defined as follows:

$$L(\rho) = \sum_{i=1}^{2} \alpha_i(\rho)L_i \tag{12}$$

with $L_i \in \mathbb{R}^{5\times 2}$

The estimation error is given as

$$e(t) = x(t) - \hat{x}(t) \tag{13}$$

Differentiating $e(t)$ with respect to time and using (7) and (11), one obtains

$$\begin{cases} \dot{e} & = \dot{x} - \dot{\hat{x}} \\ & = (A - L(\rho)C)e + B(\rho)\Delta\Phi \cdot u \\ & +(D_1 - L(\rho)D_2)\omega \\ e_z & = C_z e \end{cases} \tag{14}$$

where $\Delta\Phi = \Phi(x) - \Phi(\hat{x})$

$\Phi(x)$ satisfies the Lipschitz condition in x, $\hat{x}$, as:

$$\|\Phi(x) - \Phi(\hat{x})\| \leqslant \|\Gamma(x - \hat{x})\|, \forall x, \hat{x} \tag{15}$$

Therefore, the *LPV* observer design problem is stated below:

- The system (14) is stable for $\omega(t) = 0$
- $\|e_z(t)\|_{\mathcal{L}_2} < \gamma\|\omega(t)\|_{\mathcal{L}_2}$ for $\omega(t) \neq 0$

The extension of our previous works (Pham et al. (2019a), Pham et al. (2019b)) is stated in the following theorem that solves the LPV observer design problem.

Theorem 1. Consider the system model (7) and the observer (11) . The above design problem is solved if there exist a symmetric positive definite matrix P, a matrix Y_i with $i = 1, 2$ and positive scalar ϵ_l minimizing γ such that:

$$\begin{bmatrix} \Omega_i & PB_i & PD_1 + Y_i D_2 \\ * & -\epsilon_l I_d & 0_{n,d} \\ * & * & -\gamma^2 I \end{bmatrix} < 0 \tag{16}$$

where $\Omega_i = A_i^T P + PA_i + Y_i C + C^T Y_i^T + \epsilon_l \Gamma^T \Gamma + C_z^T C_z$

the observer vertex matrices are then $L_i = -P^{-1}Y_i$

Proof. Consider the following Lyapunov function candidate

$$V(t) = e(t)^T P e(t) \tag{17}$$

Differentiating $V(t)$ along the solution of (14) yields

$$\begin{aligned} \dot{V}(t) &= \dot{e}(t)^T P e(t) + e(t)^T P \dot{e}(t) \\ &= [(A(\rho) - L(\rho)C)e + B(\rho)\Delta\Phi \cdot u \\ &+ (D_1 - L(\rho)D_2)\omega]^T P e + e^T P[(A(\rho) - L(\rho)C)e \\ &+ B(\rho)\Delta\Phi \cdot u + (D_1 - L(\rho)D_2)\omega] \end{aligned} \tag{18}$$

For brevity, define $\eta = \begin{bmatrix} e \\ \Delta\Phi \cdot u \\ \omega \end{bmatrix}$, then one obtains

$$\dot{V}(t) = \eta^T M \eta \tag{19}$$

where

$$M = \begin{bmatrix} \Omega_1(\rho) & PB(\rho) & P(D_1 - L(\rho)D_2) \\ B(\rho)^T P & 0 & 0 \\ (D_1 - L(\rho)D_2)^T P & 0 & 0 \end{bmatrix}$$

with $\Omega_1(\rho) = (A(\rho) - L(\rho)C)^T P + P(A(\rho) - L(\rho)C)$

From (15), the following condition is obtained

$$(\Delta\Phi)^T(\Delta\Phi) \leqslant e^T \Gamma^T \Gamma e \tag{20}$$

Since $0 \leqslant u \leqslant 1$, the inequality (20) implies

$$\begin{aligned} &(\Delta\Phi \cdot u)^T(\Delta\Phi \cdot u) \leqslant e^T \Gamma^T \Gamma e \\ \Leftrightarrow &\eta^T Q \eta \leqslant 0 \end{aligned} \tag{21}$$

where $Q = \begin{bmatrix} -\Gamma^T\Gamma & 0 & 0 \\ 0 & I & 0 \\ 0 & 0 & 0 \end{bmatrix}$

In order to satisfy the objective design w.r.t. the $\mathcal{L}_2$ gain disturbance attenuation, the $\mathcal{H}_\infty$ performance index is defined as:

$$\begin{aligned} J &= e_z^T e_z - \gamma^2 \omega^T \omega \\ &= \eta^T R \eta \end{aligned} \tag{22}$$

where $R = \begin{bmatrix} C_z^T C_z & 0 & 0 \\ 0 & 0 & 0 \\ 0 & 0 & -\gamma^2 I \end{bmatrix}$

By applying the $\mathcal{S}$-procedure (Boyd et al. (1994)) to both contraints (21) and $J \geq 0$, $\dot{V}(t) < 0$ if there exists a scalar $\epsilon_l > 0$ such that

$$\begin{aligned} &\dot{V}(t) - \epsilon_l(\eta^T Q \eta) + J < 0 \\ \Leftrightarrow &\eta^T(M - \epsilon_l Q + R)\eta < 0 \end{aligned} \tag{23}$$

The condition (23) is equivalent to

$$\begin{aligned} &M - \epsilon_l Q + R < 0 \\ \Leftrightarrow &\begin{bmatrix} \Omega_1(\rho) + \epsilon_l \Gamma^T \Gamma + C_z^T C_z & PB(\rho) & P(D_1 - L(\rho)D_2) \\ B(\rho)^T P & -\epsilon_l I & 0 \\ (D_1 - L(\rho)D_2)^T P & 0 & -\gamma^2 I \end{bmatrix} < 0 \end{aligned} \tag{24}$$

Let define $Y_i = -PL_i$ and substitute (8), (12) into (24), the LMI (16) is obtained. □

4. ANALYSIS OF THE OBSERVER DESIGN

In this section, the synthesis result of the *LPV* observer is shown and some simulation scenarios are performed.

4.1 Synthesis results

In INOVE testbed available at GIPSA-lab, the control signal u (duty cycle of PWM signal) is limited in the range of $[0.01, 0.3]$, since the corresponding damper forces are enough to control the real 1/5-scaled car (in terms of improvements for passenger comfort and road holding). Therefore, applying Theorem 1 with the vertices $\underline{\rho} = 10$ and $\overline{\rho} = 100$, we obtain the $\mathcal{L}_2$ gain $\gamma = 1.7409$, $\epsilon_l = 4$ and the observer gains.

4.2 Simulation

To emphasize the effectiveness of the proposed approach, the simulations are performed using the nonlinear quarter-car model (7).

The initial conditions of the proposed design are as follows:

$$\begin{aligned} x_0 &= [0,\ 0,\ 0,\ 0,\ 0]^T \\ \hat{x}_0 &= [0.01,\ -0.1,\ 0.001,\ -0.1,\ 8]^T \end{aligned}$$

Two simulation scenarios are used to evaluate the performance of the observer as follows:

Scenario 1: The sequence of sinusoidal bumps and the control input u is constant ($u = 0.2$).

Scenario 2: An ISO 8608 road profile signal (Type C) is used and control input u is obtained from a Skyhook controller.

In order to assess the robustness of the proposed method w.r.t. uncertainties on the scheduling variable, the simulation scenarios are induced two cases: $\rho = \frac{1}{\tau(u)}$ (Nominal

case) and $\rho = \frac{1}{\tau(u)+\Delta\tau}$ (Uncertain case) where $\Delta\tau$ is a random number such that $\Delta\tau \in [-0.006, 0.006]$.

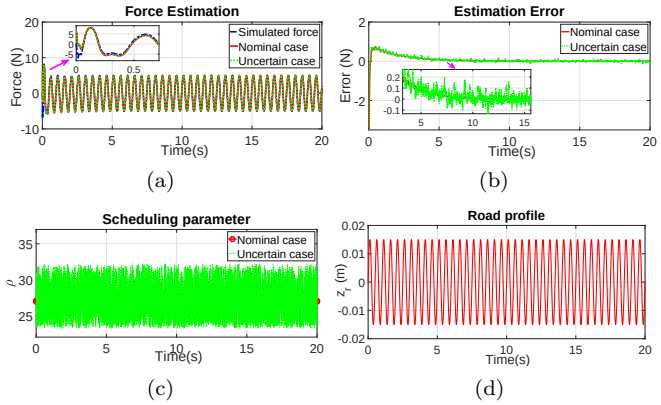


Fig. 3. Simulation scenario 1: (a) Damping force estimation, (b) Estimation error, (c) Scheduling parameter, d) road profile

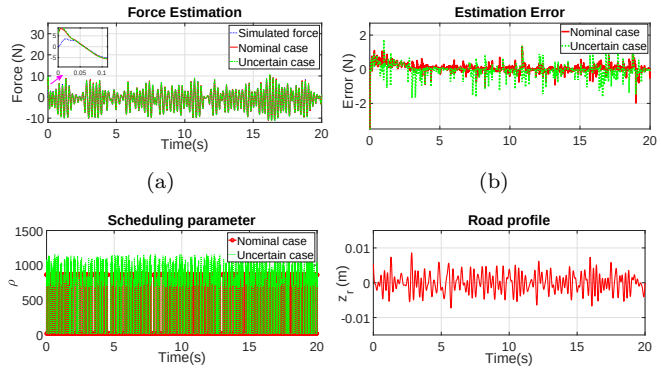


Fig. 4. Simulation scenario 2: (a) Damping force estimation, (b) Estimation error, (c) Scheduling parameter, d) road profile

Table 3. Normalized Root-Mean-Square Errors (NRMSE)-Simulation results

Scenario simulation	Nominal case	Uncertain case
Scenario 1	0.0228	0.0239
Scenario 2	0.0150	0.0164

The simulation results of two tests are shown in Fig. 3 and Fig. 4. According to Fig. 3, the performance of LPV observer to the sine wave road profile disturbance is guaranteed. Fig. 4 illustrated the robustness of the proposed LPV observer when scheduling parameter varies infinitely fast. Besides, to further illustrate the effectiveness of the proposed observer, in case, nominal and uncertain scheduling variable, Table 3 compares the normalized root-mean-square errors in the simulation scenarios 1 and 2.

5. EXPERIMENTAL VALIDATION

To experimentally assess the effectiveness of the proposed algorithm, the proposed observer is implemented on the 1/5 car scaled car INOVE available at GIPSA-lab, shown in Fig. 5.

This test-bench is equipped 4 semi-active ER suspensions, controlled in real-time using Matlab Real-Time Workshop and a host computer. The proposed observer system is implemented with the sampling period $T_s = 0.005s$. Note that the experimental platform is fully equipped with sensors to measure its vertical motion. At each corner of the system, a DC motor is used to generate the road profile.

The observer is applied for the rear-left corner using two accelerometers: the unsprung mass $\ddot{z}_{us}$ and the sprung mass $\ddot{z}_s$. For validation purpose only, the damper force sensor is used to compare the measured force with the estimated one. The block-scheme illustrates the experimental scenario of the observer (shown in Fig. 6)



Fig. 5. The experimental testbed INOVE at GIPSA-lab (see www.gipsa-lab.fr/projet/inove)

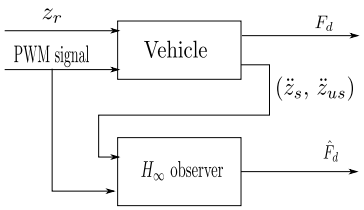


Fig. 6. Block diagram for implementation of the $\mathcal{H}_\infty$ damper force observer

Two experimental scenarios are tested as follows:

Experiment 1: The road profile is a sequence of sinusoidal bumps and the control input u is obtained from a Skyhook controller.

Experiment 2: An ISO 8608 road profile signal (Type C) is used and the control input u is obtained from a Skyhook controller.

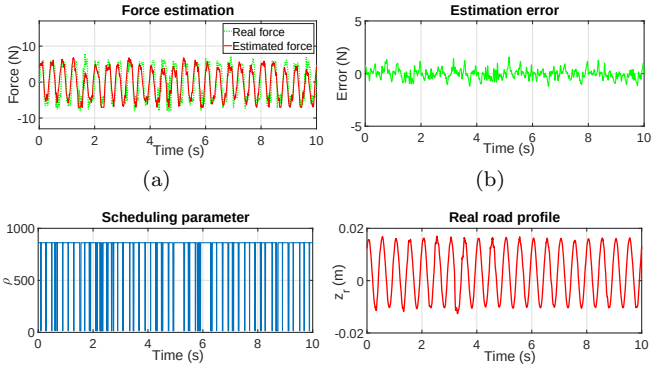


Fig. 7. Experiment 1: (a) Damping force estimation, (b) Estimation error, (c) Scheduling parameter, d) road profile

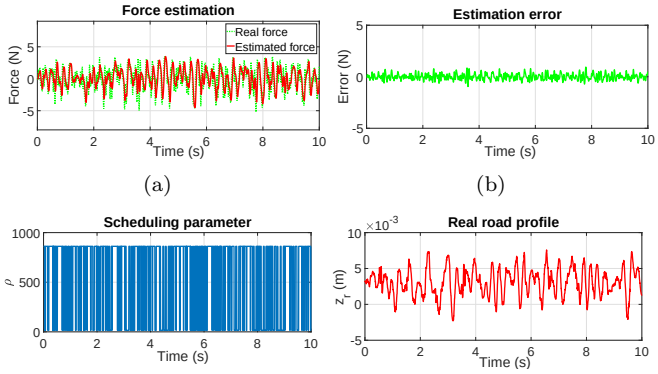


Fig. 8. Experiment 2: (a) Damping force estimation, (b) Estimation error, (c) Scheduling parameter, d) road profile

Table 4. Normalized Root-Mean-Square Errors (NRMSE)

Road Profile	NRMSE
Sinusoidal bumps	0.1021
ISO 8608 road	0.1153

The experimental results of the observer are presented in Fig. 7. The results illustrate the accuracy and efficiency of the proposed observer. To further describe this accuracy, Table 4 presents the normalized root-mean-square errors, considering the difference between the estimated and measured forces in experiment 1 and experiment 2.

6. CONCLUSION

This paper developed a polytopic *LPV* observer to estimate the damper force, using the dynamic nonlinear model of the ER damper. For this purpose, the quarter-car system is represented in LPV form by considering a phenomenological model of the damper. Based on two accelerometers, an *LPV* observer is designed, giving a good estimation result of the damping force. The estimation error is minimized accounting for the effect of unknown inputs (road profile disturbance and measurement noises) and the nonlinearity term bounded by a Lipchitz condition. Both simulation and experiment results assess the ability and the accuracy of the proposed models to estimate the damping force of the ER semi-active damper.

REFERENCES

Apkarian, P., Gahinet, P., and Becker, G. (1995). Self-scheduled h control of linear parameter-varying systems: a design example. *Automatica*, 31(9), 1251–1261.

Aubouet, S. (2010). *Semi-active SOBEN suspensions modeling and control*. Ph.D. thesis, Institut National Polytechnique de Grenoble-INPG.

Boyd, S., El Ghaoui, L., Feron, E., and Balakrishnan, V. (1994). *Linear matrix inequalities in system and control theory*, volume 15. SIAM.

Do, A.L., Sename, O., and Dugard, L. (2010). An LPV control approach for semi-active suspension control with actuator constraints. In *American Control Conference (ACC), 2010*, 4653–4658.

Estrada-Vela, A., Alcántara, D.H., Menendez, R.M., Sename, O., and Dugard, L. (2018). H_∞ observer for damper force in a semi-active suspension. *IFAC-PapersOnLine*, 51(11), 764–769.

Guo, S., Yang, S., and Pan, C. (2006). Dynamic modeling of magnetorheological damper behaviors. *Journal of Intelligent material systems and structures*, 17(1), 3–14.

Koch, G., Kloiber, T., and Lohmann, B. (2010). Nonlinear and filter based estimation for vehicle suspension control. In *Decision and Control (CDC), 2010 49th IEEE Conference on*, 5592–5597.

Koo, J.H., Goncalves, F.D., and Ahmadian, M. (2006). A comprehensive analysis of the response time of mr dampers. *Smart materials and structures*, 15(2), 351.

Nguyen, M.Q., da Silva, J.G., Sename, O., and Dugard, L. (2015). Semi-active suspension control problem: Some new results using an LPV/H_∞ state feedback input constrained control. In *Decision and Control (CDC), 2015 IEEE 54th Annual Conference on*, 863–868.

Pham, T.P., Sename, O., and Dugard, L. (2019a). Design and Experimental Validation of an H_∞ Observer for Vehicle Damper Force Estimation. In *9th IFAC International Symposium on Advances in Automotive Control (AAC 2019)*. Orléans, France.

Pham, T.P., Sename, O., and Dugard, L. (2019b). Unified H_∞ observer for a class of nonlinear Lipschitz systems: application to a real ER automotive suspension. *IEEE Control Systems Letters*, 3(4), 817 - 822.

Poussot-Vassal, C., Sename, O., Dugard, L., Gaspar, P., Szabo, Z., and Bokor, J. (2008). A new semi-active suspension control strategy through LPV technique. *Control Engineering Practice*, 16(12), 1519–1534.

Poussot-Vassal, C., Spelta, C., Sename, O., Savaresi, S.M., and Dugard, L. (2012). Survey and performance evaluation on some automotive semi-active suspension control methods: A comparative study on a single-corner model. *Annual Reviews in Control*, 36(1), 148–160.

Priyandoko, G., Mailah, M., and Jamaluddin, H. (2009). Vehicle active suspension system using skyhook adaptive neuro active force control. *Mechanical systems and signal processing*, 23(3), 855–868.

Savaresi, S.M., Poussot-Vassal, C., Spelta, C., Sename, O., and Dugard, L. (2010). *Semi-active suspension control design for vehicles*. Elsevier.

Tudon-Martinez, J.C., Hernandez-Alcantara, D., Sename, O., Morales-Menéndez, R., and Lozoya-Santos, J.d.J. (2018). Parameter-dependent H_∞ filter for LPV semi-active suspension systems. *IFAC-PapersOnLine*, 51(26), 19–24.